

## Electrospun TiO<sub>2</sub> Nanofibers in the Presence of Avocado Seed Extract

Kübra TEMİZ<sup>1</sup>, Merve ÇAPKIN YURTSEVER<sup>1\*</sup>

<sup>1</sup>Adana Alparslan Türkeş Science and Technology University, Faculty of Engineering, Department of Bioengineering, Adana, Türkiye  
(ORCID: [0000-0002-3660-3204](https://orcid.org/0000-0002-3660-3204)) (ORCID: [0000-0001-7874-4016](https://orcid.org/0000-0001-7874-4016))



**Keywords:** TiO<sub>2</sub>, Avocado seed extract, Polyvinylpyrrolidone, Electrospinning, Nanofibers.

### Abstract

Plant extracts are efficient reducing agents for the synthesis of oxide materials and can regulate fiber diameter, pore size, and phase structure in these materials because of their high organic macromolecule content. In this study, titanium tetraisopropoxide (TTIP) was used as a TiO<sub>2</sub> precursor, and PVP polymer was used as the carrier polymer for electrospinning. Avocado seed extract (ASE), which is a new and valuable source of phenolic compounds, was used for the coordination and reduction of TTIP. ASE was obtained by methanol-water extraction. The total phenolic content of ASE was calculated to be 0.16 g GAE / g dry ASE, and the total dissolved protein amount of ASE was calculated to be equivalent to 0.78 g BSA / g dry ASE. TiO<sub>2</sub>-PVP-Avocado seed extract (T/P/A) composite nanofibers were produced at different voltages, distances, and polymer concentrations. Crystalline TiO<sub>2</sub> formation was not observed in as-spun nanofibers; thus, selected nanofibers were heat treated at 500 °C for 3 h. Smooth and integrated TiO<sub>2</sub> nanofibers prepared by using 5 w% PVP at 15 kV and 15 cm distance with or without ASE were imaged by Scanning Electron Microscopy (SEM). X-ray Diffraction (XRD) patterns of heat treated TiO<sub>2</sub> nanofibers prepared in the presence of ASE crystallized mainly in anatase form. However, both anatase and rutile phases were detected in the crystalline structure of TiO<sub>2</sub> nanofibers when ASE was not used. ASE incorporation affected the phase transformation of TiO<sub>2</sub> nanofibers, indicating that the anatase-rutile ratio of TiO<sub>2</sub> nanofibers may also be controlled by the presence of ASE.

### 1. Introduction

Electrospinning is a method that utilizes electrostatic force to form polymer fibers from a wide variety of materials that contain polymers, metals, composites, and ceramics [1], [2]. Electrospinning is a cheap and sophisticated method to form nano and micro-scale fibers [3], [4]. Electrospun nanofibers have high surface area to volume ratios, and their pore sizes and diameters can easily be modified by changing the spinning parameters [5]–[7]. Electrospun nanofibers are widely used in different areas such as tissue engineering, cosmetics, filtration processes, nano-sensors, military protective clothing [8], wound healing dressings, nanocatalysts, pharmaceuticals, and probiotic encapsulation [5], [7].

Titanium dioxide has antimicrobial, photocatalytic, self-cleaning, and biocompatible

properties. Commercially pure titanium is a biologically compatible metallic material due to its surface properties, resulting in the self-deposition of stable and inert titanium dioxide [9]. Titanium tetra isopropoxide (an organic titanium precursor), TTIP, is often mixed with polyvinyl pyrrolidone (PVP) as the carrier polymer in order to synthesize TiO<sub>2</sub> nanofibers via electrospinning [10], [11]. PVP is also widely used in food additives, personal care products, pharmaceutical technology, drug delivery systems, and bioactive packaging applications [12]. In a study, TiO<sub>2</sub> nanofibers were obtained by electrospinning PVP solutions at 3 different TTIP concentrations. Smooth TiO<sub>2</sub> fibers were obtained after calcination of the electrospun nanofibrous membranes at 600 °C [13]. In another study, a water soluble form of Ti-precursor, titanium (IV) bis (ammonium lactato)

\*Corresponding author: [mcyurtserver@atu.edu.tr](mailto:mcyurtserver@atu.edu.tr)

Received: 30.09.2022, Accepted: 08.05.2023

dihydroxide (TiBALDH), was used to obtain TiO<sub>2</sub> nanofibers in the presence of PVP. The electrospun nanofibers were heat treated up to 600 °C. After heat treatment, the TiO<sub>2</sub> nanofibers preserved their integrity and showed smaller fiber diameters when compared to the diameters of as-spun nanofibers [14]. The formation of crystalline TiO<sub>2</sub> nanoparticles often requires high temperatures, starting at 400 °C. However, crystalline TiO<sub>2</sub> nanoparticles can be synthesized at low temperatures without requiring heat treatment. For this long-term aging process [15], concentrated acid solutions [16] and water soluble titanium precursors or biomolecules are used [17], [18].

The green synthesis of crystalline TiO<sub>2</sub> nanoparticles has been studied in the presence of different types of plant extracts and microorganisms. These biological samples include many types of polyphenols, flavonoids, proteins, etc., which may behave as reducing agents [19]. This environment-friendly approach both reduces the undesired effects of chemical methods and may play an important role either in the structure of TiO<sub>2</sub> nanoparticles or in their properties such as antimicrobial and photocatalytic activity [20]. In a recent study, TiO<sub>2</sub> nanoparticles were obtained at room temperature in the presence of *L. acutangula* leaf extract. Titanium sulfate was used as a precursor, and the synthesis was conducted in a water environment without a calcination step. The green synthesized nanoparticles showed very good antimicrobial activity across a wide-spectrum [21]. In addition, the beneficial effects of TiO<sub>2</sub> nanoparticles as a growth regulator and nanofertilizer-like agent on plant growth have been well described in the studies [19], [22]. The properties of green synthesized TiO<sub>2</sub> nanoparticles have been discussed in many studies; however, this study emphasizes the effects of avocado seed extract (ASE) on the morphology and crystallinity of green synthesized TiO<sub>2</sub> electrospun nanofibers for the first time.

Avocado, with its rich nutritional value, is a fruit that is frequently found on dining tables today and is also grown in Türkiye. The effects of extracts from leaves, ripe and unripe fruits, or seeds of different avocado species on microorganisms and mammalian cells, as well as their effects on nanoparticle production, were studied [23]. Avocado fruit and leaf extracts have been investigated for many years; however, ASE has recently been studied in the literature [24]. Avocado seed extracts show antioxidant, anticarcinogenic, and antimicrobial properties that make avocado seed a precious source for obtaining valuable extracts from plant waste [25], [26]. The effectiveness of the surface-active properties of polyols from ASE was examined in a

self-emulsifying drug delivery system. It was stated that the encapsulation efficiency of drugs with low water solubility, naproxen, and curcumin, was increased in the presence of ASE [27]. In another study, phospholipids obtained from avocado seeds were used to form a stable oil-in-water emulsion [28]. In the literature, no study was found in which ASE was used in the production of TiO<sub>2</sub> nanofibers.

In this study, electrospun TiO<sub>2</sub> nanofibers were synthesized in the presence of ASE. The morphology of the as-spun and heat-treated nanofibers was characterized by SEM analysis. Crystalline and chemical structures were determined by XRD and FTIR analysis, respectively.

## 2. Material and Method

### 2.1. Preparation of Avocado Seed Extract

A bacon type avocado was purchased from the commercial market. The seeds were separated from the fruit, and their shells were peeled off. Then, they were cut into small pieces. Approximately 150 g of avocado seed pieces were homogenized in a blender with 500 mL of deionized water. 500 mL of methanol was added to the blended seeds, and they were stirred at 500 rpm at room temperature (RT) for 2 h. Then, the mixture was centrifuged at 8000 rpm for 10 minutes, 3 times. The supernatant was collected and methanol was removed from the rotary evaporator at 50 °C. Water remaining in the samples was removed by freeze-drying at -80 °C (Labconco, FreeZone 2.5 Liter Benchtop Freeze Dryers). The freeze-dried ASE was stored at RT for further use.

### 2.2. Total Phenolic and Protein Content of Avocado Seed Extract

Folin Ciocalteu reagent (FC, Sigma, Germany) was used to determine the total phenolic content of ASE. Gallic acid (GA, Sigma, Germany) was used as the standard to express the phenolic content of ASE as g GA equivalent / dry weight of avocado seed extract (g GAE / g dry ASE). ASE samples were dissolved in a methanol/water (1:1) mixture at 1mg/mL concentration. The working solution for FC was prepared in ultra-pure water (UPW, 1:10 dilution). 7.5 w% Na<sub>2</sub>CO<sub>3</sub> solution was prepared in UPW. All reagents were prepared freshly just before use. Analysis was performed in triplicate on a 96-well plate. 10 µL sample or control without ASE was added to the wells. 100 µL FC working solution was added and waited for 3 min at RT. Then, 90 µL of 7.5 w% Na<sub>2</sub>CO<sub>3</sub> solution

was added, and the absorbance values of the resulting solutions were recorded at 765 nm after 1 h of incubation by a spectrophotometer (BMG Labtech, SPECTROstar Nano, Germany).

The total protein amount of ASE was determined by the Lowry protein assay. Bovine serum albumin (BSA) was used as the standard protein. A solution of 0.1 mg/mL ASE was prepared in UPW. 77  $\mu$ L of samples with or without ASE were added to the wells. Then, 108  $\mu$ L Lowry solution (it was modified from [29]) and 15  $\mu$ L FC solution (1:10 dilution in UPW) were mixed with the samples, respectively. Absorbance values were recorded at 750 nm after 1 h of incubation at RT in the dark.

### 2.3. Preparation of Electrospinning Solutions

Polyvinylpyrrolidone was supplied from Sigma (Mw 360,000 g/mol). Other chemicals were obtained from Sigma, unless stated. 0.25 g and 0.3 g of PVP were dissolved in 3.12 mL of absolute ethanol under stirring at RT overnight. 1.25 mL of acetic acid and 0.62 mL of TTIP were added to the PVP solutions, respectively, and stirred for 1.5 hours to obtain a homogeneous mixture. It is frequently seen in the literature that acetic acid is generally used to dissolve TTIP and trigger its coordination [27]–[29]. Then, 0.9 mg of ASE was added to the PVP/TTIP mixture and sonicated for 5 min at RT for a complete dissolution of the extract in the solution. The solution, including TTIP, PVP, and ASE, was taken into a 5 mL syringe with a blunt end 21-gauge needle. Electrospinning conditions are given in Table 1 and a photograph of the electrospinning apparatus is given in Figure 1 (Fytronix, electrospinning apparatus). Random nanofibers were collected for 30 min for each sample and they were dried overnight at RT. Then they were kept at RT for further analysis. The selected samples were heat treated at 500 °C for 3h (Carbolite, RHF1400). The heating ramp was 5°C/min. Nanofibers without ASE were used as control nanofibers.

### 2.4. Characterization of Electrospun Nanofibers

The surface morphology of as-spun and heat-treated nanofibers was analyzed by Scanning Electron Microscopy (SEM, FEI, Quanta 650 Field Emission).

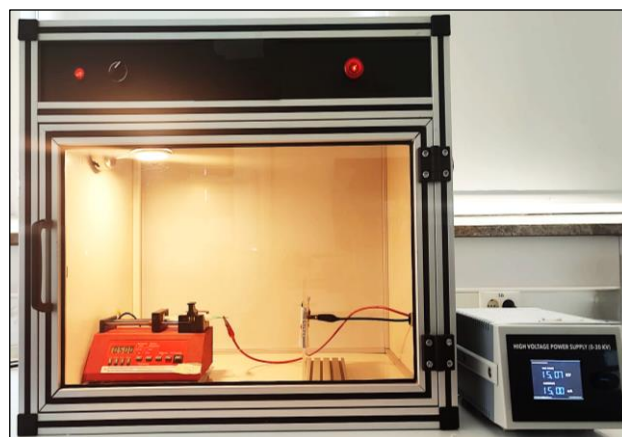


**Figure 1.** Photograph of electrospinning apparatus.

The electrospun nanofibers were sputtered with gold before imaging. The crystalline structure of TiO<sub>2</sub> was characterized by X-ray Diffraction (XRD, Rigaku MiniFlex 600) analysis. XRD patterns were fitted with the Pseudo-Voigt function. The crystallized size was calculated by using Scherrer's equation (Equation 1) by using (101) reflection of anatase, and the rutile weight percent was calculated by using (101) reflection of anatase and (110) reflection of rutile (Equation 2) [30].

$$d = \frac{k\lambda}{\beta \cdot \cos\theta} \quad (1)$$

where  $d$  is the average crystallite size (nm),  $k$  is a constant (0.9),  $\lambda$  is the X-ray wavelength (nm),  $\beta$  is the full width half maximum and  $\theta$  is the Bragg's angle.

$$x_R = 1 - \left(1 + 1.26 \frac{I_R}{I_A}\right)^{-1} \quad (2)$$

where  $x_R$  is the rutile weight fraction,  $I_R$  and  $I_A$  are the intensities of the rutile (110) peak and anatase (101) peak, respectively.

Chemical characterization was carried out by the Fourier Transform Infrared Spectroscopy (FTIR, Perkin Elmer Spectrum 2). Fiber diameters were calculated by the Image J software (NIH, USA). Statistical analysis was carried out using GraphPad Prism 9, USA. Unpaired t test was selected to compare the difference within fiber diameters.

**Table 1.** Electrospinning parameters

Polymer Concentration (w/v%)	TTIP (mL)	Ethanol (mL)	Acetic Acid (mL)	ASE/PVP (w/w%)	ASE/TTIP (w/w%)	Voltage (kV)	Distance (cm)	Flow rate (mL/h)
5 / 6	0.62	3.12	1.25	0.36 / 0.30	0.15	15 / 17	15 / 20	0.5

### 3. Results and Discussion

ASE is a precious source due to its rich nutritional and phenolic content [31], as was also demonstrated in this study. The total phenolic content of ASE was calculated to be 0.16 g GAE / g dry ASE. Total dissolved protein amount of ASE was calculated to be equivalent to 0.78 g BSA / g dry ASE. These values were within the range of the literature [24]. The effects of PVP concentration, the presence of ASE, electrospinning voltage, and the distance from the tip of the needle to the surface of the collection plate on the morphology of nanofibers were investigated. Two different polymer concentrations were selected. Uniform and homogeneously distributed nanofibers were obtained at a 5 w% PVP concentration, as shown in the SEM images (Figure 2).

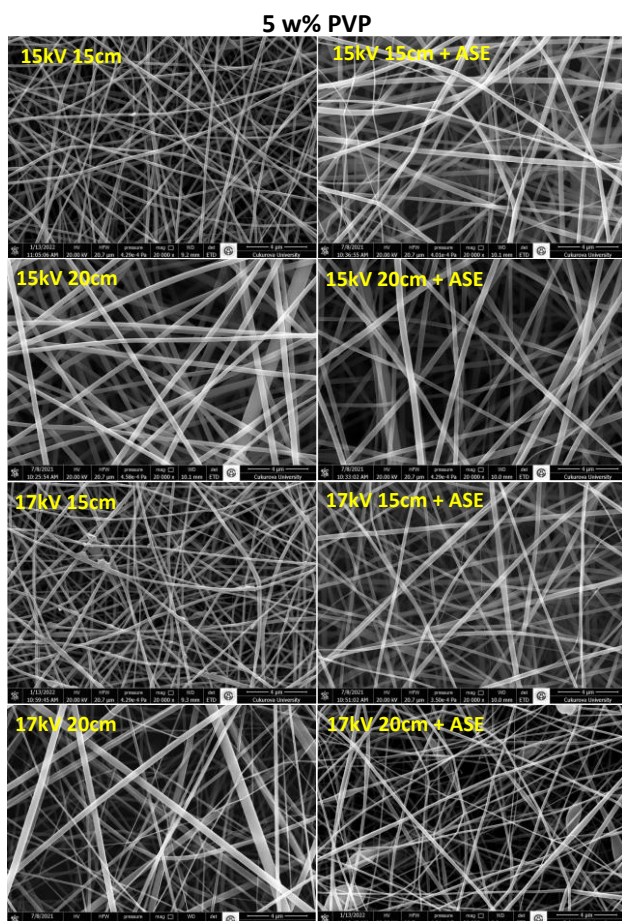


**Figure 2.** SEM images of as-spun nanofibers obtained with 5w% PVP solution, magnification: 20.000x.

Different voltage and distance values were studied for 6 a w% PVP concentration for only the fibers prepared in the presence of ASE. Wavy and non-homogenous nanofibers were obtained for the selected conditions, as seen in Figure 3. Further studies were carried out with electrospun nanofibers

prepared using a 5 w% PVP concentration. PVP polymers with different molecular weights have been used as carriers to obtain TiO<sub>2</sub> nanofibers [28], [30]. The selected concentration of carrier polymer and the solvent for electrospinning can change according to their Mw. Here, PVP with an Mw:360,000 g/mol was used at 5 w% as a carrier polymer. In the literature, high molecular weight 1,300,000 g/mol PVP was generally used for electrospinning [32], however, in a study, electrospun TiO<sub>2</sub>/PVP nanofibers were successfully obtained by using PVP with a relatively lower Mw (360,000 g/mol) [33]. Here we successfully obtained homogeneous TiO<sub>2</sub> / PVP nanofibers with PVP having Mw 360,000 g/mol.

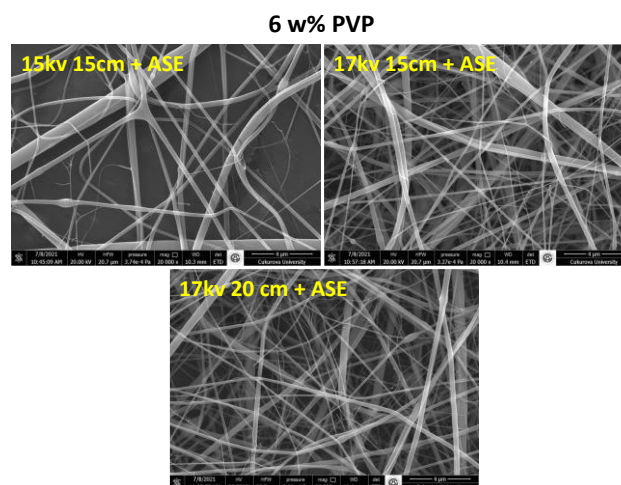


**Figure 3.** SEM images of as-spun nanofibers obtained with 6w% PVP solution, magnification: 20.000x.

Nanofibers with ASE showed different fiber morphology when compared to the control nanofibers. The average nanofiber diameter was increased; however, there were some thinner nanofibers in the structure of ASE, including groups, resulting in increased standard deviations in the nanofiber diameters. Nanofiber diameters are given in Table 2.

TiO<sub>2</sub> has three main crystalline phases named anatase, rutile, and brookite. Anatase and brookite are metastable forms that have tetragonal and orthorhombic crystalline phase structures, respectively. Rutile is the stable form of TiO<sub>2</sub>, which has a tetragonal phase structure [34]. No diffraction peaks of the crystalline phases of TiO<sub>2</sub> were observed in the XRD patterns (not shown) of the as-spun nanofibers. This result was expected for a control group without any plant extract when compared to the literature [35]. In addition, crystal growth of TiO<sub>2</sub> did not occur in the presence of ASE for the electrospinning conditions given in Table 1.

**Table 2.** Average diameters of as-spun TiO<sub>2</sub> nanofibers

Condition	Average Fiber Diameter (nm)	Condition	Average Fiber Diameter (nm)	Condition	Average Fiber Diameter (nm)
5 w% PVP - ASE		5 w% PVP + ASE		6 w% PVP + ASE	
15kV, 15cm	163.4 ± 45.6	15kV, 15cm	214.7 ± 83.6	15kV, 15cm	257.5 ± 184.4
15kV, 20cm	297.4 ± 69.4	15kV, 20cm	274.9 ± 83.5	17kV, 15cm	215.1 ± 101.3
17kV, 15cm	149.6 ± 48.5	17kV, 15cm	195.1 ± 68.9	17kV, 20cm	178.9 ± 77.9
17kV, 20cm	189.6 ± 16.2	17kV, 20cm	167.4 ± 58.6		

The formation of crystalline phases of TiO<sub>2</sub> in a mild environment depends on the precursor of TiO<sub>2</sub>. It was shown that anatase TiO<sub>2</sub> can be obtained from TTIP in the presence of acetic acid and water at RT after one week of aging [36]. Here, electrospinning solutions were prepared just before use to prevent precipitation. The interaction time between ASE and TTIP may not be enough to start the crystallization of TiO<sub>2</sub> at RT.

The selected nanofibers (15 kv, 15 cm, 5 w% PVP) were heat-treated at 500 °C for 3 hours in order to crystallize TiO<sub>2</sub>. The heat-treated nanofibers retained their integrity, as seen in the SEM images (Figure 4). PVP polymer (Mw:360,000) loses more than 95% of its weight below 500 °C heat treatment [36], thus these nanofibers may be referred to as TiO<sub>2</sub> nanofibers as the new structure is nearly 100% TiO<sub>2</sub>.

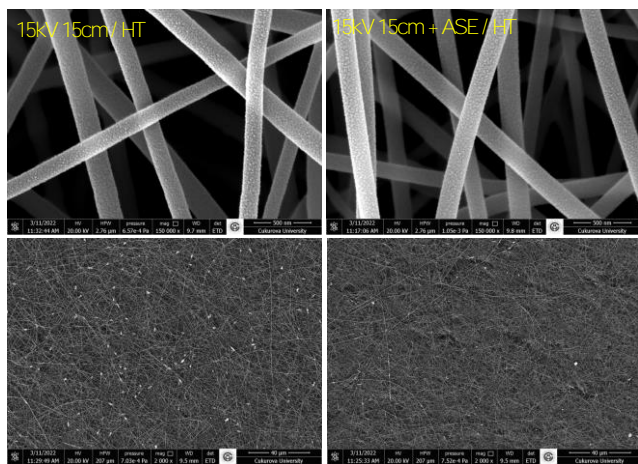


**Figure 4.** SEM images of heat treated (HT) nanofibers obtained with the electrospinning of 5 w% PVP including solution. Magnifications of the images are 150,000x and 2,000x.

There was less beading formation in TiO<sub>2</sub> nanofibers when they were obtained in the presence of ASE. The distribution of fiber diameter was changed after heat treatment. TiO<sub>2</sub> nanofibers with

ASE showed smaller diameter and narrower size distribution,  $181 \pm 2$  nm, when compared to the

diameters of control TiO<sub>2</sub> nanofibers without ASE,  $203 \pm 4$  nm ( $p < 0.01$ , \*\*).

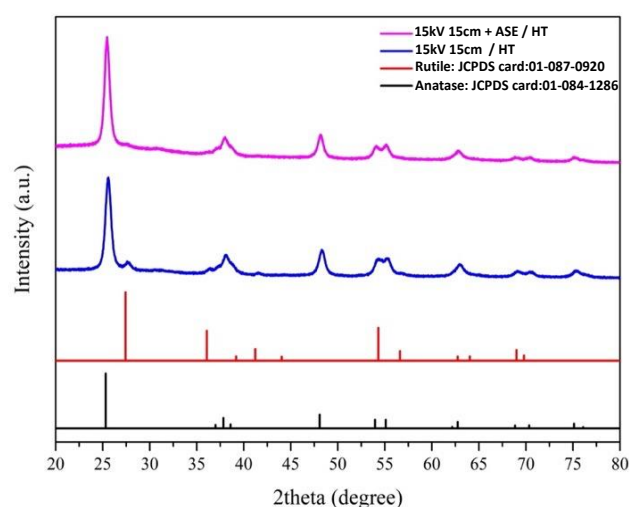


**Figure 5.** XRD patterns of nanofibers with or without ASE (15 kV, 15 cm, 5 w% PVP) heat treated at 500 °C for 3 hours.

The crystalline properties of the heat-treated nanofibers were determined by XRD analysis. Figure 5 shows the XRD patterns of selected composite nanofibers at the specified conditions. In the presence of ASE, the main phase was found to be anatase with trace amounts of rutile phase (corresponding to the JCPDS cards given in the figure; JCPDS: Joint Committee on Powder Diffraction Standards). However, without ASE, the crystalline structure is still dominated by the anatase phase, but with relatively higher amounts of the rutile phase (about 9 w%). This finding indicated that ASE has a significant effect on the phase evolution of TiO<sub>2</sub>. The phase transformation from anatase to rutile could possibly be hindered by organic molecules in the ASE [30]. The crystallite sizes for the control and ASE-containing samples were determined to be 11.6 and 12.6 nm, respectively. It is known that anatase is more

photocatalytically active than rutile, whereas rutile absorbs light in a wider wavelength range than anatase. Therefore, the presence of both anatase and rutile phases in the nanostructure may contribute to the photocatalytic activity. The XRD patterns of the heat-treated nanofibers revealed that an optimization in the anatase-rutile ratio in the nanostructure can be realized by the modification of the ASE amount in the as-spun nanofibers along with the heat treatment temperature, as discussed for metal dopants in the literature [37].

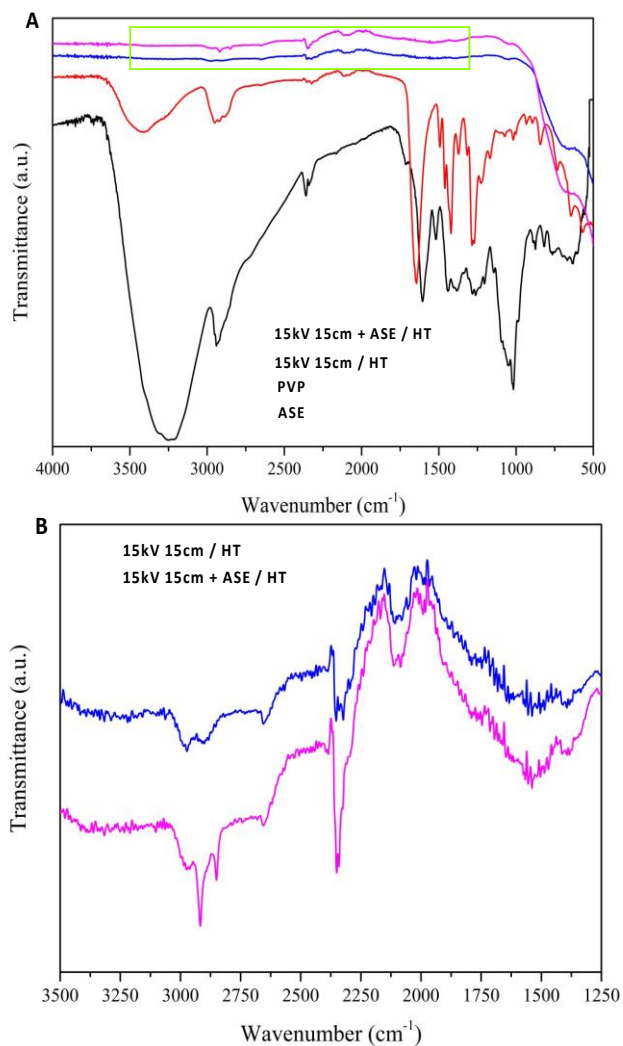


**Figure 6.** A) FTIR spectra of PVP, ASE and nanofibers heat treated (HT) at 500°C for 3 hours. B) The magnified image of FTIR spectra between 1250-3500  $\text{cm}^{-1}$ .

The bending vibration of Ti-O-Ti bonds in the  $\text{TiO}_2$  lattice was observed in the range of 500-600  $\text{cm}^{-1}$  [39] by FTIR analysis, as seen in Figure 6. Characteristic bands of PVP at 1644  $\text{cm}^{-1}$  and 1345  $\text{cm}^{-1}$  were attributed to the vibration of the C=O bond and the stretching vibration of the C-N bond, respectively [40]. The strong peak at 1025  $\text{cm}^{-1}$  in

ASE was attributed to the vibrations of C-O stretching in ester groups. The wide peak at 3414  $\text{cm}^{-1}$  was attributed to the O-H stretching [41]. Here, it was expected for the polymer to burn completely; however, there are still some peaks that may be related to PVP, ASE, or  $\text{TiO}_2$  interaction. These peaks were between 2250-3000  $\text{cm}^{-1}$  and the intensities of the peaks were higher for nanofibers with ASE when compared to the control nanofibers. ASE is an organic mixture of plants, so it was also expected to burn after heat treatment. However, the peaks between 2250-3000  $\text{cm}^{-1}$  may be an indication that organic molecules are not completely burned. On the other hand, specific bonds for PVP and ASE mostly disappeared after heat treatment.

#### 4. Conclusion and Suggestions

Pure  $\text{TiO}_2$  nanofiber networks can be prepared by the electrospinning method. Herein, the green synthesis and characterization of electrospun  $\text{TiO}_2$  nanofibers in the presence of avocado seed extract (ASE) were performed. As-spun  $\text{TiO}_2$  nanofibers with or without ASE were amorphous, whereas crystalline nanofibers were obtained after heat treatment. ASE has a significant effect on the phase evolution of heat-treated  $\text{TiO}_2$  nanofibers. Anatase is the main phase in the crystalline structure of  $\text{TiO}_2$  nanofibers with or without ASE. However, 9 w% rutile phase was detected in  $\text{TiO}_2$  nanofibers without ASE which was at trace amounts in  $\text{TiO}_2$  nanofibers with ASE. In addition, smaller diameter fibers were obtained in the presence of ASE. Fiber diameter and crystalline structure are important parameters that may affect the photocatalytic activity, antimicrobial, and biocompatibility properties of the synthesized material. Further studies are needed to show how ASE will affect the functional properties of  $\text{TiO}_2$  nanofibers.

#### Acknowledgement

This study was supported by The Scientific and Technological Research Council of Türkiye (TÜBİTAK) in context of the project TÜBİTAK 2209A/ 1919B012000903.

#### Contributions of the authors

Kübra Temiz contributed to the literature review, experiments, evaluation of data and article writing, while Merve Çapkın Yurtsever contributed to the formation of ideas, evaluation of the data, article writing and editing.

**Statement of Research and Publication Ethics**

The study is complied with research and publication ethics.

**Conflict of Interest Statement**

There is no conflict of interest between the authors.

**References**

- [1] N. Z. A. Al-Hazeem, "Nanofibers and Electrospinning Method," in *Novel Nanomaterials - Synthesis and Applications*, InTech, 2018. doi: 10.5772/intechopen.72060.
- [2] A. ElenaOprea, A. Ficai, and E. Andronescu, "Electrospun nanofibers for tissue engineering applications," in *Materials for Biomedical Engineering: Nanobiomaterials in Tissue Engineering*, 2019, pp. 77–95. doi: 10.1016/B978-0-12-816909-4.00004-X.
- [3] A. Luzio, E. V. Canesi, C. Bertarelli, and M. Caironi, "Electrospun polymer fibers for electronic applications," *Materials*, vol. 7, no. 2. pp. 906–947, 2014. doi: 10.3390/ma7020906.
- [4] R. S. Bhattarai, R. D. Bachu, S. H. S. Boddu, and S. Bhaduri, "Biomedical applications of electrospun nanofibers: Drug and nanoparticle delivery," *Pharmaceutics*, vol. 11, no. 1. MDPI AG, Jan. 01, 2019. doi: 10.3390/pharmaceutics11010005.
- [5] N. Bhardwaj and S. C. Kundu, "Electrospinning: A fascinating fiber fabrication technique," *Biotechnology Advances*, vol. 28, no. 3. pp. 325–347, May 2010. doi: 10.1016/j.biotechadv.2010.01.004.
- [6] M. Rahmati *et al.*, "Electrospinning for tissue engineering applications," *Progress in Materials Science*, vol. 117. Elsevier Ltd, Apr. 01, 2021. doi: 10.1016/j.pmatsci.2020.100721.
- [7] H. Yu, W. Liu, D. Li, C. Liu, Z. Feng, and B. Jiang, "Targeting delivery system for *Lactobacillus plantarum* based on functionalized electrospun nanofibers," *Polymers (Basel)*, vol. 12, no. 7, pp. 1–12, Jul. 2020, doi: 10.3390/polym12071565.
- [8] Z. M. Huang, Y. Z. Zhang, M. Kotaki, and S. Ramakrishna, "A review on polymer nanofibers by electrospinning and their applications in nanocomposites," *Compos Sci Technol*, vol. 63, no. 15, pp. 2223–2253, 2003, doi: 10.1016/S0266-3538(03)00178-7.
- [9] C. N. , Elias, J. H. C. , Lima, and R. et al. Valiev, "Biomedical applications of titanium and its alloys," *JOM*, vol. 60, pp. 46–49, 2008.
- [10] O. Kéri, P. Bárdos, S. Boyadjiev, T. Igricz, Z. K. Nagy, and I. M. Szilágyi, "Thermal properties of electrospun polyvinylpyrrolidone/titanium tetraisopropoxide composite nanofibers," *J Therm Anal Calorim*, vol. 137, no. 4, pp. 1249–1254, Aug. 2019, doi: 10.1007/s10973-019-08030-0.
- [11] K. Ghosal, C. Agatemor, Z. Špitálský, S. Thomas, and E. Kny, "Electrospinning tissue engineering and wound dressing scaffolds from polymer-titanium dioxide nanocomposites," *Chemical Engineering Journal*, vol. 358, pp. 1262–1278, Feb. 15, 2019. doi: 10.1016/j.cej.2018.10.117.
- [12] F. Çalloğlu C and Kesici Güler H, "Çevreci Çözücüler ile Polivinilpirolidon Nanolif Üretimi," *Süleyman Demirel Üniversitesi Fen Edebiyat Fakültesi Fen Dergisi*, pp. 352–366, Nov. 2019, doi: 10.29233/sdufeffd.589516.
- [13] S. Kiennork, R. Nakhwong, R. Chueachot, and U. Tipparach, "Preparation and Characterization of Electrospun TiO<sub>2</sub> Nanofibers via Electrospinning," in *Integrated Ferroelectrics*, Sep. 2015, vol. 165, no. 1, pp. 131–137. doi: 10.1080/10584587.2015.1063915.
- [14] O. V. Otieno *et al.*, "Synthesis of TiO<sub>2</sub> nanofibers by electrospinning using water-soluble Ti-precursor," *J Therm Anal Calorim*, vol. 139, no. 1, pp. 57–66, Jan. 2020, doi: 10.1007/s10973-019-08398-z.
- [15] K. Qi and J. H. Xin, "Room-temperature synthesis of single-phase anatase TiO<sub>2</sub> by aging and its self-cleaning properties," *ACS Appl Mater Interfaces*, vol. 2, no. 12, pp. 3479–3485, Dec. 2010, doi: 10.1021/am1005892.
- [16] K. Fischer *et al.*, "Low-temperature synthesis of anatase/rutile/brookite TiO<sub>2</sub> nanoparticles on a polymer membrane for photocatalysis," *Catalysts*, vol. 7, no. 7, Jul. 2017, doi: 10.3390/catal7070209.
- [17] M. Taran, M. Rad, and M. Alavi, "Biosynthesis of TiO<sub>2</sub> and ZnO nanoparticles by *Halomonas elongata* IBRC-M 10214 in different conditions of medium," *BioImpacts*, vol. 8, no. 2, pp. 81–89, 2018, doi: 10.15171/bi.2018.10.

- [18] Rajakumar G *et al.*, “Solanum trilobatum extract-mediated synthesis of titanium dioxide nanoparticles to control *Pediculus humanus capitis*, *Hyalomma anatolicum anatolicum* and *Anopheles subpictus*,” *Parasitol Res*, vol. 113, no. 2, pp. 469–479, 2014, doi: 10.1007/s00436-013-3676-9.
- [19] P. K. Dikshit *et al.*, “Green synthesis of metallic nanoparticles: Applications and limitations,” *Catalysts*, vol. 11, no. 8, Aug. 01, 2021. doi: 10.3390/catal11080902.
- [20] M. Nadeem *et al.*, “The current trends in the green syntheses of titanium oxide nanoparticles and their applications,” *Green Chem Lett Rev*, vol. 11, no. 4, pp. 492–502, Oct. 2018, doi: 10.1080/17518253.2018.1538430.
- [21] D. Anbumani *et al.*, “Green synthesis and antimicrobial efficacy of titanium dioxide nanoparticles using *Luffa acutangula* leaf extract,” *J King Saud Univ Sci*, vol. 34, no. 3, Apr. 2022, doi: 10.1016/j.jksus.2022.101896.
- [22] V. Rodríguez-González, C. Terashima, and A. Fujishima, “Applications of photocatalytic titanium dioxide-based nanomaterials in sustainable agriculture,” *Journal of Photochemistry and Photobiology C: Photochemistry Reviews*, vol. 40, pp. 49–67, Sep. 01, 2019. doi: 10.1016/j.jphotochemrev.2019.06.001.
- [23] B. R. Athaydes *et al.*, “Avocado seeds (*Persea americana* Mill.) prevents indomethacin-induced gastric ulcer in mice,” *Food Research International*, vol. 119, pp. 751–760, May 2019, doi: 10.1016/j.foodres.2018.10.057.
- [24] F. J. Segovia, G. I. Hidalgo, J. Villasante, X. Ramis, and M. P. Almajano, “Avocado seed: A comparative study of antioxidant content and capacity in protecting oil models from oxidation,” *Molecules*, vol. 23, no. 10, Sep. 2018, doi: 10.3390/molecules23102421.
- [25] A. Ochoa-Zarzosa *et al.*, “Bioactive Molecules From Native Mexican Avocado Fruit (*Persea americana* var. *drymifolia*): A Review”, doi: 10.1007/s11130-021-00887-7/Published.
- [26] J. E. Pineda-Lozano, A. G. Martínez-Moreno, and C. A. Virgen-Carrillo, “The Effects of Avocado Waste and Its Functional Compounds in Animal Models on Dyslipidemia Parameters,” *Frontiers in Nutrition*, vol. 8, Feb. 16, 2021. doi: 10.3389/fnut.2021.637183.
- [27] N. Ahmed *et al.*, “Avocado-derived polyols for use as novel co-surfactants in low energy self-emulsifying microemulsions,” *Sci Rep*, vol. 10, no. 1, Dec. 2020, doi: 10.1038/s41598-020-62334-y.
- [28] L. C. B. Züge, H. A. Maieves, J. L. M. Silveira, V. R. da Silva, and A. de P. Scheer, “Use of avocado phospholipids as emulsifier,” *LWT - Food Science and Technology*, vol. 79, pp. 42–51, Jun. 2017, doi: 10.1016/j.lwt.2017.01.013.
- [29] O. H. Lowry, N. J. Rosebrough, A. L. Farr, and R. J. Randall, “Protein measurement with the Folin phenol reagent\*”, *J Biol Chem*. 1951 Nov;193(1):265-75.
- [30] H. A. Yurtsever and M. Çiftçioglu, “The effect of rare earth element doping on the microstructural evolution of sol-gel titania powders,” *J Alloys Compd*, vol. 695, pp. 1336–1353, Feb. 2017, doi: 10.1016/j.jallcom.2016.10.275.
- [31] L. Henry, L. N. Henry, U. Yonah Mtaita, and C. C. Kimaro, “Nutritional efficacy of avocado seeds”, *Global Journal of Food Science and Technology*, vol. 3, pp. 192-196, August, 2015.
- [32] Z. S. Tang, N. Bolong, I. Saad, and J. L. Ayog, “The Morphology of Electrospun Titanium Dioxide Nanofibers and Its Influencing Factors” *MATEC Web Conf.*, vol. 47, p. 01020 doi: 10.1051/mateconf/20164701020.
- [33] S. Mirmohammad Sadeghi, M. Vaezi, A. Kazemzadeh, and R. Jamjah, “Morphology enhancement of TiO<sub>2</sub>/PVP composite nanofibers based on solution viscosity and processing parameters of electrospinning method,” *J Appl Polym Sci*, vol. 135, no. 23, Jun. 2018, doi: 10.1002/app.46337.
- [34] L. E. Oi, M. Y. Choo, H. V. Lee, H. C. Ong, S. B. A. Hamid, and J. C. Juan, “Recent advances of titanium dioxide (TiO<sub>2</sub>) for green organic synthesis,” *RSC Advances*, vol. 6, no. 110., pp. 108741-108754, 2016. doi: 10.1039/c6ra22894a.
- [35] T. Soitong and S. Wongsanmai, “Characteristic and preparation of TiO<sub>2</sub>/PVP nanofiber using electrospinning technique,” in *Key Engineering Materials*, 2019, vol. 798 KEM, pp. 223–228. doi: 10.4028/www.scientific.net/KEM.798.223.
- [36] K. Qi and J. H. Xin, “Room-temperature synthesis of single-phase anatase TiO<sub>2</sub> by aging and its self-cleaning properties,” *ACS Appl Mater Interfaces*, vol. 2, no. 12, pp. 3479–3485, Dec. 2010, doi: 10.1021/am1005892.

- [37] H. A. Yurtsever and M. Çiftçioğlu, “The effect of powder preparation method on the artificial photosynthesis activities of neodymium doped titania powders,” *Int J Hydrogen Energy*, vol. 43, no. 44, pp. 20162–20175, Nov. 2018, doi: 10.1016/j.ijhydene.2018.08.185.
- [38] S. Huang, L. Zhou, M. C. Li, Q. Wu, Y. Kojima, and D. Zhou, “Preparation and properties of electrospun poly (vinyl pyrrolidone)/cellulose nanocrystal/silver nanoparticle composite fibers,” *Materials*, vol. 9, no. 7, Jul. 2016, doi: 10.3390/ma9070523.
- [39] S. Al-Taweel, H. Saud, S. S. Al-Taweel, and H. R. Saud, “New route for synthesis of pure anatase TiO<sub>2</sub> nanoparticles via ultrasound-assisted sol-gel method,” *Available online www.jocpr.com Journal of Chemical and Pharmaceutical Research*, vol. 8, no. 2, pp. 620–626, 2016, [Online]. Available: www.jocpr.com
- [40] Y. C. Hung, S. C. Hsieh, S. R. Hou, J. Y. Kung, C. M. Tang, and C. J. Chang, “In vivo evaluation of pvp-gelatin-chitosan composite blended with egg-yolk oil for radiodermatitis,” *Applied Sciences*, vol. 11, no. 21, Nov. 2021, doi: 10.3390/app112110290.
- [41] Kamaruddin, D. Edikresnha, I. Sriyanti, M. M. Munir, and Khairurrijal, “Synthesis of Polyvinylpyrrolidone (PVP)-Green Tea Extract Composite Nanostructures using Electrohydrodynamic Spraying Technique,” in *IOP Conference Series: Materials Science and Engineering*, May 2017, vol. 202, no. 1. doi: 10.1088/1757-899X/202/1/012043.